



CHORUS

This is the accepted manuscript made available via CHORUS. The article has been published as:

Effect of the Magnus force on skyrmion relaxation dynamics

Barton L. Brown, Uwe C. Täuber, and Michel Pleimling
Phys. Rev. B **97**, 020405 — Published 10 January 2018

DOI: [10.1103/PhysRevB.97.020405](https://doi.org/10.1103/PhysRevB.97.020405)

The effect of the Magnus force on skyrmion relaxation dynamics

Barton L. Brown,^{1,2} Uwe C. Täuber,^{1,2} and Michel Pleimling^{1,2,3}

¹*Department of Physics, Virginia Tech, Blacksburg, VA 24061-0435, USA*

²*Center for Soft Matter and Biological Physics, Virginia Tech, Blacksburg, VA 24061-0435, USA*

³*Academy of Integrated Science, Virginia Tech, Blacksburg, VA 24061-0405, USA*

(Dated: December 28, 2017)

We perform systematic Langevin molecular dynamics simulations of interacting skyrmions in thin films. The interplay between Magnus force, repulsive skyrmion-skyrmion interaction and thermal noise yields different regimes during non-equilibrium relaxation. In the noise-dominated regime the Magnus force enhances the disordering effects of the thermal noise. In the Magnus-force-dominated regime, the Magnus force cooperates with the skyrmion-skyrmion interaction to yield a dynamic regime with slow decaying correlations. These two regimes are characterized by different values of the aging exponent. In general, the Magnus force accelerates the approach to the steady state.

Magnetic skyrmions, particle-like spin textures encountered in many magnetic thin films and bulk materials with broken inversion symmetry and strong spin-orbit coupling under a weak applied magnetic field [1–4], have recently been observed at room temperature [5, 6]. This opens many possible avenues for applications in spintronics such as data storage [7, 8] and logic [9] devices due to the ultra-low current densities required to move these topologically protected spin textures.

Recent computational [10, 11] and experimental [12, 13] evidence suggests that a particle-like treatment of skyrmions is valid in certain regimes. Using Thiele’s approach [14, 15], which treats skyrmions as rigid point-like particles, equations of motion can be derived [10] that lend themselves to in-depth numerical simulations of interacting skyrmion systems. A similar treatment has been used to derive equations of motion for vortices in type-II superconductors [16, 17], and the resulting equations are in fact quite similar to those for skyrmions [18], except for the Magnus force which is usually negligible in vortex dynamics. The Magnus force acts normal to the drift velocity of the skyrmion and can therefore cause orbits or spiraling trajectories. Recent progress has focused on the steady-state properties and dynamical phase transitions of driven skyrmions moving in an environment with random quenched disorder [11, 19, 20] or on a substrate [21–23].

As applications become more widespread it will be important to develop a more complete understanding of the relaxation dynamics of interacting skyrmions. Exploiting the particle equations of motion and the resulting coarse-grained framework, we probe in the following relaxation processes of many interacting skyrmions far from equilibrium. Our main emphasis is to gain a better understanding of how the interplay between the Magnus force, the repulsive skyrmion-skyrmion interaction, and thermal fluctuations affect the non-equilibrium relaxation properties of skyrmion systems.

In the absence of defects or strong noise, skyrmions crystallize into a triangular lattice configuration, see Fig. 1, due to the mutual repulsive force between them. Non-

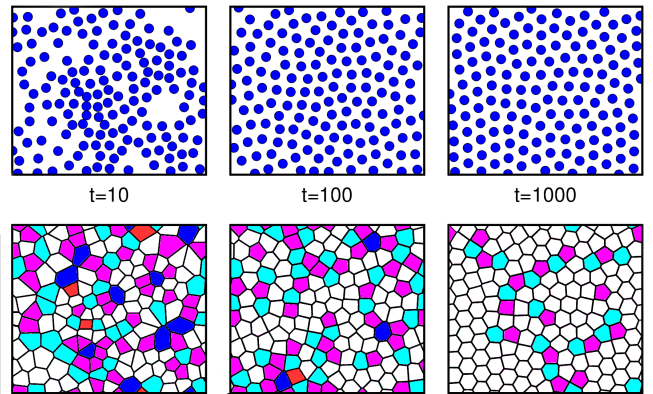


FIG. 1: A system of interacting skyrmions prepared in a disordered initial state at $t = 0$ evolves over time into a triangular configuration. Voronoi diagrams constructed from the particle positions are shown in the bottom row. In a perfect triangular lattice each region associated with a particle would form a regular hexagon. At early times the Voronoi lattice is dominated by defects (polygons that are not hexagons), with the number of defects decreasing over time. Polygons have between four and eight sides and are colored in red, magenta, white, cyan, or blue from least to greatest side number.

equilibrium relaxation kinetics of ordering systems are often paired with physical aging phenomena. A many-body system is said to undergo physical aging if the following three properties are satisfied [24]: (1) the relaxation towards equilibrium is slow, i.e. non-exponential; (2) time-translation invariance is broken; and (3) dynamical scaling is present. Prominent examples of physical aging can be found in coarsening systems (including spin glasses and magnets), polymer glasses, and growth processes, to name but a few [25–27]. As revealed by numerous theoretical and experimental studies, physical aging is best studied through the investigation of two-time quantities [24].

We consider interacting skyrmions moving on a two-dimensional surface under the rigid structure approxi-

mation, where deformations of the internal spin structure are taken to be negligible so that the skyrmions are treated as point-like particles. Recent experiments point to the validity of this particle-like treatment [12, 13]. The motion of N interacting skyrmions is modeled according to a set of Langevin equations derived from Thiele's approach [14, 15, 28] and defined in terms of the skyrmion drift velocities $\mathbf{v}_i(t)$ and positions $\mathbf{r}_i(t)$

$$\eta \mathbf{v}_i = \mathbf{F}_i^M + \mathbf{F}_i^s + \mathbf{f}, \quad (1)$$

where $i = 1, \dots, N$ labels the N different skyrmions, whereas η is the damping coefficient. $\mathbf{F}_i^M = \beta \hat{\mathbf{z}} \times \mathbf{v}_i$ is the Magnus force, whose strength can be adjusted by changing the value of the parameter β . The Magnus force, which acts in the direction perpendicular to the skyrmion's velocity, does not contribute to the energy of the system and therefore does not break detailed balance. Still, as shown in the following, the presence of the Magnus force significantly affects the transient dynamical properties of a system of interacting skyrmions.

The repulsive skyrmion-skyrmion interaction in (1) has the form (as determined through a numerical study [10]) $\mathbf{F}_i^s = \sum_{i \neq j} F_0^s K_1(r_{ij}/\xi) \hat{\mathbf{r}}_{ij}$ where $K_1(y)$ is the modified Bessel function of the second kind, $\hat{\mathbf{r}}_{ij} = \mathbf{r}_{ij}/|\mathbf{r}_{ij}| = (\mathbf{r}_i - \mathbf{r}_j)/|\mathbf{r}_i - \mathbf{r}_j|$ is the unit vector pointing from skyrmion j to skyrmion i , and ξ is the healing length. This force decays exponentially for $r_{ij}/\xi \gg 1$. Finally, the last term on the right side is thermal white noise obeying $\langle f_\mu(t) \rangle = 0$ and $\langle f_\mu(t) f_\nu(t') \rangle = \sigma \delta_{\mu\nu} \delta(t - t')$, with $\sigma = 2\eta k_B T$ and $\mu, \nu = 1, 2$ [29]. No driving currents are included here and the pinning due to defects are considered to be negligible.

In the following simulations we take the skyrmion interaction coefficient $F_0^s = 1$. We also apply a constraint on the system in terms of the coefficients η and β , namely that $\eta^2 + \beta^2 = 1$ [21, 22]. This constraint ensures that the average magnitude of the velocity of a free skyrmion is independent of the Magnus force. We also ran simulations without this constraint (not shown) and verified that the same qualitative behavior is obtained as that discussed in the following. We choose units such that the healing length $\xi = 1$ [10].

We consider in the following systems of size $\frac{2}{\sqrt{3}} 36 \times 36$ with periodic boundary conditions that allow for the skyrmions to form at equilibrium a triangular lattice. We tested that the skyrmions in the absence of noise indeed settle into this triangular configuration. The non-equilibrium simulations reported below have been done with $N = 149$ skyrmions (which corresponds to a coverage of 10%). We checked that our results are robust against changing system sizes and/or coverage, as long as the particle picture remains valid. As revealed by many other studies of non-equilibrium relaxation processes [24], results obtained for some system size are representative of much larger systems as long as the system is not yet close to its steady state. We assume that the system is

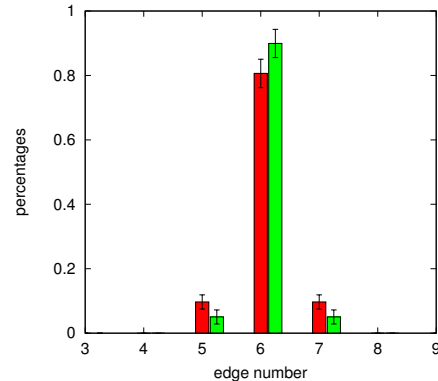


FIG. 2: Edge statistics of Voronoi diagrams generated from the skyrmion positions at time $t = 800$ and noise strength $\sigma = 0$, with the Magnus force either turned off (red/left) or on with $\beta/\eta = 5$ (green/right). An increase of the probability to observe six-sided polygons is seen in simulations with a non-zero Magnus force, indicating a faster relaxation into equilibrium in the presence of this force. The data result from averaging over 150,000 independent runs.

initially in a disordered state where the skyrmions are located at random positions in our two-dimensional system. The system is then allowed to relax for $t > 0$ at the temperature T (or, equivalently, at a given value of σ) following the Langevin dynamics discussed above and quantities are measured as a function of time.

A first indication of the Magnus force's impact on relaxation processes can be garnered from a statistical analysis of Voronoi maps like those shown in Fig. 1. In Fig. 2 we compare for the case without noise the edge statistics for Voronoi diagrams obtained from simulations with (in green at the right) and without (in red at the left) the Magnus force at time $t = 800$ since preparation of the system. With the addition of the Magnus force, six-sided domains become more likely than without, indicating that the presence of the Magnus force facilitates the crystallization into the triangular lattice. This is a consequence of the fact that rearrangements of particles are easier due to the dynamical bending of the moving particles' trajectories. It is this facilitation of collective motion that allows the system to find new, and quicker, paths towards the steady state.

For a more detailed investigation of the relaxation process and the related aging phenomena we turn to two-time quantities, such as the two-time density autocorrelation function, that have been shown to provide valuable insights into these processes [24]. Over time the repulsive skyrmion-skyrmion interaction tends to maximize the skyrmions' average nearest neighbor distance. As a result the skyrmions move away from their random initial positions, causing the decay of the density autocorrelation function. In order to capture these changes we follow Ref. [30] and set at time s a circular area with radius r (the data discussed below have been obtained

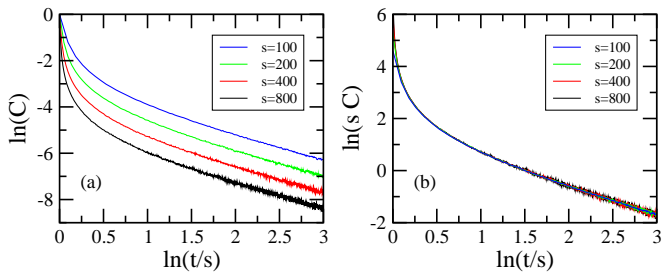


FIG. 3: (a) The two-time autocorrelation (2) of a system of non-interacting skyrmions, for various waiting times, s . The trajectories are completely determined by thermal fluctuations causing the skyrmions to perform random walks. This results in a simple aging scaling behavior with an aging exponent $b = 1$, see Eq. (3), as shown in panel (b). The data displayed in this figure, which result from averaging over 8000 independent runs, have been obtained for $\sigma = 0.1$ and $\beta/\eta = 0$, but the observed scaling is independent of the values of these parameters.

for $r = 0.08$, but none of the observed features change when choosing a different, albeit similar, value for r) at the location of each skyrmion. At time $t > s$, we count the number of skyrmions still in their circles, generating the occupation numbers $n_i(t)$, with $n_i = 0$ or 1 (of course $n_i(t = s) = 1$ by construction). This quantity is then averaged over the N different skyrmions as well as over many initial conditions and realizations of the noise to produce the two-time autocorrelation

$$C(t, s) = \left\langle \frac{1}{N} \sum_{i=1}^N n_i(t) n_i(s) \right\rangle. \quad (2)$$

A test case, which will help us to understand the relaxation properties of the full problem, is provided by switching off the interactions between skyrmions, see Fig. 3. In that case the skyrmions perform independent random walks, and it is expected that the two-time autocorrelation function (2) displays a simple aging scaling form [24]

$$C(t, s) = s^{-b} f_C(t/s), \quad (3)$$

with the aging exponent b and a scaling function $f_C(y)$ that only depends on the time ratio $y = t/s$. As shown in Fig. 3, the data obtained for different waiting times s display a perfect scaling with $b = 1$. We observe the same scaling for all values of σ , both in the absence or presence of the Magnus force. Indeed the Magnus force, which corresponds to a non-zero value of β , serves only to rotate the skyrmions in the plane but leaves the statistical properties of the random walks unaltered.

We supplement the results from the density autocorrelations by measuring also the time-dependent average nearest-neighbor distance

$$D(t) = \left\langle \frac{1}{N} \sum_i \min_{i \neq j} r_{ij} \right\rangle \quad (4)$$

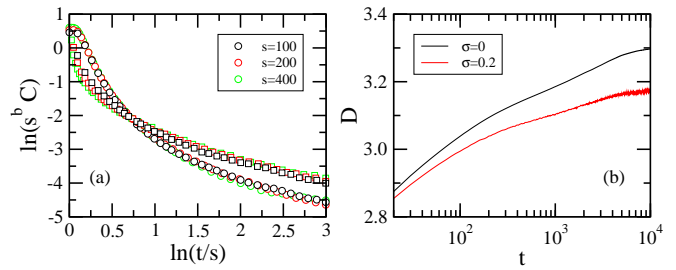


FIG. 4: (a) Scaled two-time autocorrelation function for different waiting times s and (b) average nearest-neighbor distance for the two noise strengths $\sigma = 0$ (circles in (a) and black line in (b)) and $\sigma = 0.2$ (squares in (a) and red line in (b)) in the absence of the Magnus force. The scaling exponent b in (a) varies with the noise strength σ , with $b = 0.10$ for $\sigma = 0$ and $b = 0.30$ for $\sigma = 0.2$. At higher values of σ , skyrmions are on average driven further away from their preferred positions within the lattice which yields lower values of $D(t)$. For $\sigma = 0$ the system still contains imperfections at the end of our runs, with D being slightly smaller than the equilibrium value. The data for the autocorrelation result from averaging over a few thousands independent runs, whereas for $D(t)$ we averaged over a few hundred independent realizations.

from random initial conditions. In a regular triangular lattice where each of the N sites is occupied by a skyrmion, the distance between two neighboring skyrmions is $l_\Delta = \frac{2}{\sqrt{3N}}L$. For the system studied in this work this yields $l_\Delta \approx 3.4$. The distance $D(t)$, which approaches the value l_Δ only at very late stages of the ordering process, provides a time-dependent length scale that may encode additional interesting details of the relaxation of the system [31].

The relaxation of interacting skyrmions is much more complex than that of free particles. As discussed in Figs. 4 and 5, the interplay between skyrmion interaction, thermal fluctuations, and Magnus force yields aging scaling with non-universal (i.e. dependent on the strength of the different terms) aging exponents. To disentangle the different contributions, we first discuss in Fig. 4 the behavior in the presence of interactions and thermal noise alone, before considering in addition the effects of the Magnus force in Fig. 5.

In the absence of pinning disorder our system of interacting skyrmions evolves toward the regular triangular lattice. Thermal noise, however, prohibits the system to reach the perfect triangular lattice, which instead settles for moderate noise levels into a partially ordered state where most of the particles fluctuate around their ground state positions. Neglecting the Magnus force, this yields an average distance between skyrmions that is slightly reduced compared to that measured in the absence of noise, see Fig. 4b. Further increasing σ increases this effect until for very large noise levels (corresponding to large temperatures) the skyrmions behave effectively like free skyrmions as long as they are not too close. Conse-

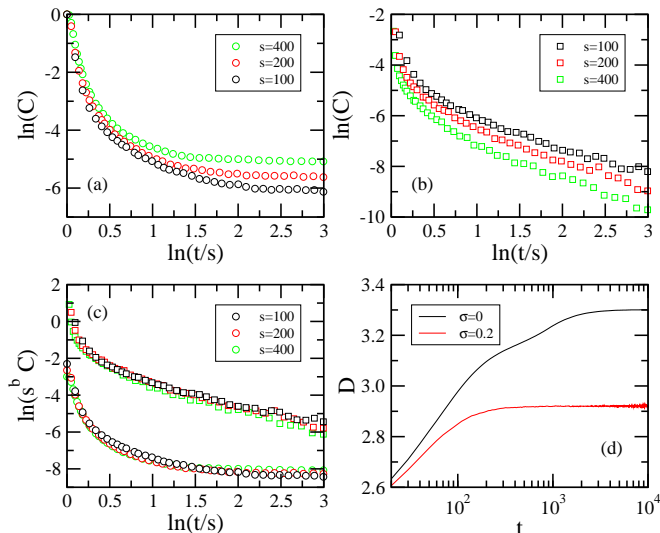


FIG. 5: Unscaled two-time autocorrelation function as a function of t/s for different values of s in the presence of a Magnus force with $\beta/\eta = 5$: (a) $\sigma = 0$ (circles) and (b) $\sigma = 0.2$ (squares). In (a) the data sets are ordered from bottom to top when increasing the waiting time s , whereas in (b) it is the other way round. (c) Scaled two-time autocorrelations ($\sigma = 0$: circles; $\sigma = 0.2$: squares) and (d) average nearest neighbor distances for the same two cases. The value of the aging exponent changes sign when decreasing σ , being $b = 0.60$ for $\sigma = 0.2$ and $b = -0.50$ for $\sigma = 0$.

Without Magnus Force		With Magnus Force	
$\beta/\eta = 0$		$\beta/\eta = 5$	
σ	b	σ	b
∞	1.0	∞	1.0
0.5	0.45	0.5	0.95
0.2	0.30	0.2	0.60
0.1	0.20	0.1	-0.20
0.0	0.10	0.0	-0.50

TABLE I: Measured values of the aging scaling exponent with and without the Magnus force.

quently, we expect for large values of σ a scaling behavior close to that displayed in Fig. 3, with more pronounced deviations showing up the smaller the value of σ is. As shown in Fig. 4a and Table I, this is indeed the case, with the value of the aging exponent b decreasing monotonically until it reaches the minimal value $b = 0.10$ in the absence of noise.

As already mentioned, a general property of the Magnus force is to accelerate relaxation toward the final state. One way to see that is to compare Figs. 4b and 5d that show the time-dependent average distance between skyrmions. In the presence of the Magnus force $D(t)$ approaches much faster a plateau-like behavior that indicates the proximity to the final state. Focusing first on the case of large values of σ , we remark that in this noise-dominated regime the Magnus force enhances the effects of the thermal noise, resulting in disordered states

characterized by a much smaller value of D at long times than that encountered if the Magnus force is negligible (see the data for $\sigma = 0.2$). This is also readily seen in the scaling of the autocorrelation, see Fig. 5c and Table I, where the aging scaling exponent b is much larger for $\sigma = 0.2$ and $\sigma = 0.5$ when the Magnus force is present. Remarkably, for $\sigma = 0.5$ the value $b = 0.95$ is already very close to the value $b = 1$ for the case $\sigma = \infty$ where thermal noise completely dominates the skyrmion interaction.

A second regime of interest is that where the Magnus force dominates the thermal noise, yielding predominantly curved trajectories. Comparing in Figs. 5a and 5b the unscaled autocorrelation function for $\sigma = 0$ and $\sigma = 0.2$, we note an inversion of the order of the data sets as a function of the waiting time. For $\sigma = 0.2$, and this is the same for the cases without the Magnus force discussed in Figs. 3 and 4, the larger the waiting time is, the smaller the value of C is for a given value of t/s , which yields a positive aging exponent $b > 0$. In contrast to this, for $\sigma = 0$ the autocorrelation for a fixed value of t/s is larger for larger waiting times, which then yields a *negative* aging exponent $b < 0$, see Table I. This remarkable change indicates that in the Magnus-force-dominated regime the complicity of the Magnus force and the skyrmion-skyrmion interaction yields states that are increasingly correlated the closer the system gets to the steady state.

Our study of interacting skyrmions has yielded important insights into relaxation processes for situations where the particle picture prevails. These processes are heavily influenced by the interplay of the Magnus force, the repulsive skyrmion-skyrmion interactions, and the thermal noise. In general, the Magnus force accelerates the relaxation process, allowing the system to approach the steady state much faster than in the absence of this velocity-dependent force. Our study reveals two different regimes, one dominated by thermal noise, the other dominated by the Magnus force. In the former regime the Magnus force enhances the effects of the noise, resulting in final states with increased disorder, as measured by the significantly lower value of the average distance between skyrmions. In the regime dominated by the Magnus force, the cooperation between this force and the skyrmion-skyrmion interaction yields an increase of the correlations between successive configurations. The change in regime is signaled by a change of the sign of the aging exponent b . It will be interesting to see whether these different regimes can be identified experimentally in studies of interacting skyrmions at different temperatures.

This research was supported by the US Department of Energy, Office of Basic Energy Sciences, Division of Materials Sciences and Engineering under Grant No. DE-FG02-09ER46613.

-
- [1] U. K. Röbber, A. N. Bogdanov, and C. Pfeleiderer, *Nature* **442**, 797 (2006).
- [2] S. Mühlbauer, B. Binz, F. Jonietz, C. Pfeleiderer, A. Rosch, A. Neubauer, R. Georgii, and P. Böni, *Science* **323**, 915 (2009).
- [3] X. Z. Yu, Y. Onose, N. Kanazawa, J. H. Park, J. H. Han, Y. Matsui, N. Nagaosa, and Y. Tokura, *Nature* **465**, 901 (2010).
- [4] X. Z. Yu, N. Kanazawa, Y. Onose, K. Kimoto, W. Z. Zhang, S. Ishiwata, Y. Matsui, and Y. Tokura, *Nat. Mater.* **10**, 106 (2011).
- [5] S. Woo, K. Litzius, B. Krüger, M.-Y. Im, L. Caretta, K. Richter, M. Mann, A. Krone, R. M. Reeve, M. Weigand, P. Agrawal, I. Limesh, M.-A. Mawass, P. Fischer, M. Kläui, and G. S. D. Beach, *Nat. Mater.* **15**, 501 (2016).
- [6] O. Boule, J. Vogel, H. Yang, S. Pizzini, D. de Souza Chaves, A. Locatelli, T. O. Mentes, A. Sala, L. D. Budaprebeanu, O. Klein, M. Belmeguenai, Y. Roussigné, A. Stashkevich, S. M. Chérif, L. Aballe, M. Foerster, M. Chshiev, S. Auffret, I. M. Miron, and G. Gaudin, *Nat. Mater.* **15**, 501 (2016).
- [7] A. Fert, V. Cros, and J. Sampaio, *Nat. Nanotechnol.* **8**, 152 (2013).
- [8] N. S. Kiselev, R. Schäfer, and U. K. Röbber, *J. Physics D* **44**, 39 (2011).
- [9] X. Zhang, M. Ezawa, and Y. Zhou, *Scientific Reports* **5**, 9400 (2015).
- [10] S.-Z. Lin, C. Reichhardt, C. D. Batista, and A. Saxena, *Phys. Rev. B* **87**, 214419 (2013).
- [11] C. Reichhardt and C. J. Olson Reichhardt, *New J. Phys.* **18**, 095005 (2016).
- [12] W. Jiang, X. Zhang, G. Yu, W. Zhang, X. Wang, M. B. Jungfleisch, J. E. Pearson, X. Cheng, O. Heinonen, K. L. Wang, Y. Zhou, A. Hoffmann, and S. G. E. te Velthuis, *Nat. Phys.* **13**, 162 (2017).
- [13] S. Pöllath, J. Wrilld, L. Heinen, T. N. G. Meier, M. Kronseider, L. Tutsch, A. Bauer, H. Berger, C. Pfeleiderer, J. Zweck, A. Rosch, and C. H. Back, *Phys. Rev. Lett.* **118**, 207205 (2017).
- [14] A. A. Thiele, *Phys. Rev. Lett.* **30**, 230 (1973).
- [15] N. Nagaosa and Y. Tokura, *Nat. Nanotechnol.* **8**, 899 (2013).
- [16] D. R. Nelson and V. M. Vinokur, *Phys. Rev. B* **48**, 13060 (1993).
- [17] H. Assi, H. Chaturvedi, U. Dobramysl, M. Pleimling, and U. C. Täuber, *Mol. Simul.* **42**, 1401 (2016).
- [18] C. J. Olson Reichhardt, S. Z. Lin, D. Ray, and C. Reichhardt, *Physica C* **503**, 52 (2014).
- [19] C. Reichhardt, D. Ray, and C. J. Olson Reichhardt, *Phys. Rev. Lett.* **114**, 217202 (2015).
- [20] S. A. Díaz, C. J. Olson Reichhardt, D. P. Arovas, A. Saxena, and C. Reichhardt, *Phys. Rev. B* **96**, 085106 (2017).
- [21] C. Reichhardt, D. Ray, and C. J. Olson Reichhardt, *Phys. Rev. B* **91**, 104426 (2015); *New J. Phys.* **17**, 073034 (2015).
- [22] C. Reichhardt and C. J. Olson Reichhardt, *Phys. Rev. B* **92**, 224432 (2015); *Phys. Rev. B* **94**, 094413 (2016); *Phys. Rev. B* **95**, 014412 (2017).
- [23] X. Ma, C. J. Olson Reichhardt, and C. Reichhardt, *Phys. Rev. B* **95**, 104401 (2017).
- [24] M. Henkel and M. Pleimling, *Non-Equilibrium Phase Transitions, Volume 2: Ageing and Dynamical Scaling Far From Equilibrium* (Springer, Heidelberg, 2010).
- [25] M. Henkel, M. Pleimling, and R. Sanctuary (Editors), *Ageing and the Glass Transition*, Lecture Notes in Physics **716** (Springer, Berlin, 2007).
- [26] H. Rieger, *J. Phys. A: Math. Gen.* **26**, L615 (1993).
- [27] M. Henkel, J. D. Noh, and M. Pleimling, *Phys. Rev. E* **85**, 030102(R) (2012).
- [28] Such a strongly interacting many-body system cannot be adequately captured by a Fokker-Planck equation.
- [29] As discussed in Ref. [10], values of the dimensionless parameters in the Langevin equation (1) can be derived from experimental data. For example, for MnSi a temperature of 15 K corresponds to the value $\sigma = 0.1$.
- [30] M. Pleimling and U. C. Täuber, *Phys. Rev. B* **84**, 174509 (2011).
- [31] M. Pleimling and U. C. Täuber, *J. Stat. Mech.* (2015) P09010.